BRL
1133
c.1A
REFERENCE COPY

QA

BRL
1133

BRL

REPORT NO. 1133
JUNE 1961

CORRELATED ELECTRICAL AND OPTICAL MEASUREMENTS OF EXPLODING WIRES

F. D. Bennett
H.S. Burden
D. D. Shear

BRL
1133

TECHNICAL LIBRARY
U S ARMY ORDNANCE
ABERDEEN PROVING GROUND, MD.
ORDBG-TL

Department of the Army Project No. 503-03-009
Ordnance Management Structure Code No. 5210.11.140

BALLISTIC RESEARCH LABORATORIES
ABERDEEN PROVING GROUND, MARYLAND

ASTIA AVAILABILITY NOTICE

Qualified requestors may obtain copies of this report from ASTIA.

TECHNICAL LIBRARY
U S ARMY ORDNANCE
ABERDEEN PROVING GROUND, MD.
ORDBG-TL

B A L L I S T I C R E S E A R C H L A B O R A T O R I E S

REPORT NO. 1133

JUNE 1961

CORRELATED ELECTRICAL AND OPTICAL MEASUREMENTS OF EXPLODING WIRES

F. D. Bennett
H. S. Burden
D. D. Shear

Exterior Ballistics Laboratory

TECHNICAL LIBRARY
U S ARMY ORDNANCE
ABERDEEN PROVING GROUND, MD.
ORDBG-TL

Department of the Army Project No. 503-03-009
Ordnance Management Structure Code No. 5210.11.140

A B E R D E E N P R O V I N G G R O U N D, M A R Y L A N D

B A L L I S T I C R E S E A R C H L A B O R A T O R I E S

REPORT NO. 1133

FDBennett/HSBurden/DDShear/sec
Aberdeen Proving Ground, Md.
June 1961

CORRELATED ELECTRICAL AND OPTICAL MEASUREMENTS OF EXPLODING WIRES

ABSTRACT

Description is given of a high-resolution streak camera and of an experimental method whereby streak camera records and electrical measurements of exploding wires may be accurately correlated in time. Composite data together with derived values of resistance, power and energy are given for 4 and 5 mil Cu wires at several voltages. These data are compared with the experimental and theoretical results of other workers. From the comparison a coherent model of the exploding wire phenomenon emerges which differs in some details, particularly those having to do with electric arc formation, from models proposed earlier. The transfer of energy from electrical to fluid mechanical form is discussed as are problems having to do with formation of the shock waves.

Page intentionally blank

Page intentionally blank

Page intentionally blank

TABLE OF CONTENTS

1. INTRODUCTION

In this paper we extend our study of the matched-circuit exploding wire phenomenon with an analysis of current and voltage measurements in the electrical circuit, correlated in time with measurements of light intensity and with high-resolution, rotating-mirror, streak-camera photographs. Other authors have presented data aimed at correlating optical and electrical measurements, and in particular Reithel et. al.[1] employ methods quite similar to ours. We believe our method of time correlation represents an improvement over any previously used; furthermore our high-speed streak camera data reveal some new features of the explosion not seen before. Part of the reason for these novelties lies in our consideration only of exploding wires nearly matched to the electrical parameters of the circuit in the sense defined in an earlier paper[2]. This means that energy transfer from condenser to exploding wire occurs mainly at first current peak; and, given sufficient condenser energy, the explosion proceeds rapidly and completely. Under these conditions the current dwell is absent and if the matching is sufficiently good so that condenser energy is expended early, arc discharge along the wire axis after the expansion does not occur.

In what follows we (1) describe briefly the optical and electrical techniques employed, (2) exhibit streak photographs delineating typical, matched-wire explosions, (3) introduce a reasonable assumption which allows precise time-correlation of electrical and optical records (of which examples are given), (4) show calculated curves depicting wire resistance, instantaneous power, and electrical energy absorbed by the wire and finally, (5) discuss comparisons which can be made between wire input energy and shock wave energy derived from similarity flow theory.

2. EXPERIMENTAL

2.1 High-Speed, Rotating-Mirror Camera.

Streak cameras employing rapidly rotating mirrors to sweep the image on the film plane have been employed in many studies of short-duration, transient phenomena. For the principles of design of a camera with sub-microsecond time resolution and small f number, we refer to a recent paper by Brauer and Hansen[3]. Because the exploding wire phenomenon produces so much light a camera with large light gathering power is not necessary. And in order to make visible the non-luminous phases of the phenomenon, an efficient source of backlighting must be provided. Thus for our purposes a compromise design is desirable which will reject much of the self-lighting, yet utilize to the maximum the backlighting provided by a pulsed light source. The camera layout is sketched in Figure 1. The train of events involved in obtaining a streak photograph is initiated by the operator who allows a pulse from the photocell, receiving light reflected off the back mirror surface, to switch on the backlighting and after a delay of 1 μsec the exploding wire itself. Backlighting is furnished by a B-H6, mercury-arc lamp subjected to a 15 μsec duration square wave formed by a simulated transmission line made of lumped L-C elements. Collimated light from the source aperture is limited by the 10 mil slit and brought to focus by the camera lens on the 1 cm^2 face of a cubic stainless steel mirror, whence it diverges to the film drum. Most of the light from the wire explosion which would be imaged by the camera lens on the film drum, falls outside the aperture defined by the mirror face and is lost.

An approximate analysis based on geometrical optics has been made of the photographic speed of the rotating mirror camera relative to that of the backlighting system. We find theoretically that the effective speed of the backlighting system can never exceed that of the objective lens and rotating mirror. In unfavorable cases the speed of the backlighting system may be much less than that of the camera with the results that much detail may be lost where the object is highly luminous and undue burden is put on the intensity of the source of backlighting. For purposes of comparison in

the present system the equivalent f number of the collimating system is only 2% larger than that of the camera, which itself is f/130 with respect to the exploding wire.

The camera lens is a two element objective of 50" focal length designed originally to be used with a 10" interferometer and to have a flat image field practically free of distortion at 1:1 magnification. In the present camera the magnification is established experimentally at the value of 0.9 by measuring the image of a precision grid placed in the position of the wire.

Because of the limiting aperture of the mirror only a small central portion of the lens, about 1" in diameter, is effective in forming the image of the explosion. For this reason, the depth of focus is about 2 cm and a circular film drum is used rather than the limacon necessary where precise image focusing is desired. Because of the long lever arm of this arrangement, at a mirror speed of 1800 rps (which is 85% of the maximum safe speed) the ideal, theoretical time resolution is about 10 nano-sec (1 nano-sec = 10^{-9} sec). Direct microscopic measurement in the image plane with blue light and with the mirror stationary shows a maximum apparent slit width of about 0.34 mm or 13 mils, a value in good agreement with estimates of the expected diffraction. Thus actual time resolution may conceivably be no better than 14 nano-sec even neglecting mirror distortion and air compressibility effects (both expected to be small). It is clear that this time resolution is far above the ultimate limit, for rotating mirror cameras, of 1/4 nano-sec quoted by Courtney-Pratt[4]. As will be seen later the experimental streak records apparently resolve events closer in time by a factor of nearly 2 than the practical limit of 14 nano-sec given above. This indicates that either the method of calculations based on apparent slit width is too conservative or that other effects intervene.

2.2 Streak Pictures

Figure 2 shows the front half of two representative streak records obtained with the high-speed camera. In both of these, the shadow of the wire at constant diameter is followed by an expansion region about 0.1 μsec in duration. This is a feature unresolved in our previous pictures[5] both

because the earlier camera speed is slower by a factor of 25 and because the early expansion is obscured in the bright flash which immediately follows. Measurements show the radius of the expansion to be approximately linear with time. Next a brief transition region occurs marked by the beginning of a burst of light, following which the boundary traces a parabolic path with time. At about 1.5 μsec the shock wave and contact surface can be seen to separate, after which the cloud of dispersed metal expands more slowly than the shock and asymptotically reaches a constant radius. Meanwhile the shock propagates outward and weakens rapidly until Mach number originally 10 or higher at the point of separation drops to less than 3 at the end of the trace. The flow region between the shock and contact surface exhibits many small discontinuities which represent either non-uniformities in the expanding shock front projected onto the film plane, or compressive disturbances in the interior flow.

Figure 2(c) shows an enlargement of the tip section of the explosion to illustrate the sharpness of both the onset of luminosity and of the change in rate of expansion. Because this transition region appears to be the shortest phenomenon resolved by the camera, estimates from several film records set the duration of the transition region in the range of 8-12 nano-sec. If we adopt the mean value of 10 nano-sec then it appears that the actual camera resolution is close to the theoretical value but 40% smaller than the more conservative experimental value given above.

2.3 Electrical Measurements

Current and voltage in the exploding wire circuit are measured by a low resistance, series element and a high resistance parallel element respectively. The current measuring resistor, shown schematically in Figure 3, is constructed according to a design of Park[6]. The resistive portion consists of a hollow cylinder of Nichrome V at the shorted end of a coaxial stub which is connected in series with the exploding wire; and, in fact, located at the common ground connected to one of the wire binding posts. The dc resistance of the shunt is 1.054×10^{3} ohms and its calculated inductive reactance at 1/2 mc is less than 5% of the resistance; thus the impedance is larger than the resistance

by less than 0.2%. The shunt is designed for currents up to a maximum of 10^5 amps at which value it would presumably be crushed by magnetic pinch forces. Isolation of the voltage sensing probe from the main current field is achieved by the coaxial design. Resistance under steady state conditions is nearly independent of frequency below 1.5 mc since the thickness of the hollow cylinder is 0.7 of the skin depth at this frequency.

Voltage is measured across the wire by a tapped divider made of carbon resistors. The voltage ratio of the divider, as seen by the terminated, 100 Ω transmission line at the scope, is 106 within about 2%. This error estimate is based on voltage ratio measurements made using square waves at frequencies of 1/2 and 1 mc.

A schematic diagram of the electrical circuit is given in Figure 4. Figure 5 shows the exploding wire unit itself. Lowest on the pedestal one sees the triggering spark gap which is normally enclosed in a light-tight cardboard housing, then the wire binding posts with the shunt mounted on the left and finally the voltage divider with shielded cable leading off to the scopes. The adjustable vertical slit is in the background.

Measurements of the circuit damping made with the exploding wire replaced by a copper strap show the circuit inductance and resistance to be 0.24 μhy and 0.15 ohm respectively. The inductance of 1/2" length of 5 mil wire estimated from handbook tables is .014 μhy. The combined capacitance is 0.485 μfd. The condensers themselves are each nominally 1/4 μfd and rated at 15 kv.

Finally, light output from the exploding wire is measured by a 929 phototube in a simple series circuit with a 1000 Ω resistance and 350 v battery. The rise time of this arrangement to 90% full scale is about 45 nano-sec.

The general technique of the combined measurements may be described as follows. Current-time and voltage-time traces are recorded photographically by one of the dual-beam scopes while voltage-time and light intensity versus time are recorded by the other. When the voltage curves from the two separate

records are carefully matched, a time correlation between the three measured quantities viz., current, voltage and light output is achieved. The train of events is initiated by the observer who triggers the auxiliary spark-gap. The main gap breaks down, the wire explosion occurs and simultaneously the data records are taken. Calibration experiments of the scopes indicate vertical deflection accuracy to about 2% of full scale. The horizontal sweep shows a considerable nonlinearity in the beginning interval of 50 nano-sec; however because of the delay line in the oscilloscope, the most nonlinear portion is not used and the time mapping is better then 1% in the second half of the sweep and not worse than 6% in the significant portions of the first half. Since this sweep error is systematic, it can be removed by correcting the time scale. Such correction has been made in the quantitative curves given below.

3. RESULTS

3.1 Typical Wire Explosions

Combined streak and electrical data on a common time base for a 4 mil Cu wire, 1.2 cm long, exploded at 10.8 kv are shown in Figure 6(a). The four oscilloscope traces under the streak picture represent voltage across the wire, relative light output of the wire, voltage repeated and current in the circuit. Because of difficulty in setting triggering levels, the delay between the two scopes is about 0.1 μsec; and although the sweep rates agree to within 0.7%, without other clues an accurate time correlation would be difficult if not impossible. The simultaneous voltage records offer means for accurate alignment.

Inspection of the voltage curves shows two distinctive features, viz., (1) the slight break in the rising portion and (2) the voltage peak. We disregard the small oscillations on the rising current curve and the falling portion of both the current and voltage curves. These seem to be the irreducible remnants of parasitic oscillations in external circuits completed by stray capacitance between the condenser cans and portions of the screen-wire cage. Damping resistors connected between the cage and cans largely remove the oscillations.

By aligning both the breaks and the peaks in the voltage curves on a Telereader or other large field comparator, the two oscilloscope records can be adjusted to agree within about 10 nano-sec. Thus precise comparisons between the electrical records are possible.

The electrical and optical records can now be aligned by comparison between the light output curve and the streak picture. The streak photograph shows a well-defined, sharp tipped luminous streak just behind the initial expansion of the wire. The photo-tube record shows three distinct parts, a slow rise in light output from the wire terminated by a very steep rise to high values followed in turn by an approximately exponential decay. If we assume what now seems obvious, viz., that the photo-tube rise and the luminous streak represent the same burst of light, an alignment of the optical and electrical records is possible.

TECHNICAL LIBRARY
U S ARMY ORDNANCE
ABERDEEN PROVING GROUND, MD.
ORDBG TL

A densitometer trace of the film taken along the axis of the wire through the luminous region yields a density curve very similar in shape to the light output curve. Close examination shows in some instances a break in the steep rising portion of both curves. By matching the breaks and peaks of light output with those of the densitometer trace, and by matching film and densitometer trace, the electrical and optical records can be correlated to within 30 nano-sec. Such a correlation has been made for the data of this paper. We turn now from problems of time correlation to those of interpretation of various features of the curves.

3.2 Interpretation of the Oscilloscope Records

The initial slow rise of light output has already been remarked. No corresponding glow of the wire during this interval can be seen on the streak photograph mainly because of the rejection of direct light by the camera. Light output during the linear expansion phase has been noticed previously in the slower explosion of 10 mil Pd wires observed with either direct lighting only, or direct and reflected lighting[7]. In the referenced pictures the wire is seen faintly glowing during the linear expansion but not before, and becomes a brilliant light source with the onset of the parabolic expansion and shock wave. Our present data show the wire to be glowing during the current rise and at least 0.2 μsec before the linear expansion. We may tentatively identify this glow as the visible radiation associated with ohmic heating of the wire. It seems unlikely that we have to deal here with the type of glow discharge reported by Tucker[8]; for the voltage across the wire appears to be too small to produce any visible electrical effect. This conclusion may be justified by noting that the voltage remains nearly constant at 800 v during the first half of the slow light build-up. Assuming this voltage to be inductive and equal $L(dI/dt)_{t=o}$ one finds $L \doteq .03$ μhy. This inductance is about twice that estimated for the cold wire itself and may be attributed to the combined effects of the wire and the unavoidable flux linkages of the voltage divider and leads. Thus only about half the induced voltage can actually appear across the wire; our estimates give a field of 325 v/cm, a value about 10^2 below the breakdown potential for air at 1 atm; thus supporting our contention that the cause is thermal radiation and not electric discharge.

The assumption that the initial voltage rise is caused by the combined inductance of the wire and voltage measuring circuit makes possible a correction to the voltage data by subtracting $L(dI/dt)_t$ from corresponding points of the raw voltage curve. The resulting plot of voltage vs time should more closely represent true IR drop across the wire. The correction is most accurate over the first half trace before the wire explodes, because wire inductance decreases as its diameter increases. For a 5 mil wire expanded four diameters the decrease is 30%. Thus by later times the correction may be too large by nearly 15%, but is relatively insignificant because total voltage is comparatively large and the slope of the current curve may be near zero. The correction is numerically largest on the steep descending portion of the current curve. Here the voltage is near its maximum; so maximum error in the correction, caused by overestimating the now unknown wire inductance, is still less than 1% of the peak voltage. This inductive voltage correction has been applied to all subsequent plotted voltage curves.

Figure 6(b) shows composite optical and electrical data for a 1.2 cm, 5 mil Cu wire exploded at 12.4 kv. While certain peculiarities are evident that distinguish these data from those of Figure 6(a), we wish at this stage to draw attention to the similar trends of voltage, current and light output in the two sets of data. The general features of our wire explosions as shown in Figures 6(a) and 6(b), appear to be the following: (a) linear initial current rise, (b) initial inductive jump in voltage, caused by both wire and measuring circuit inductance, followed by a gradually increasing voltage as wire resistance increases, (c) a slight break on the voltage curve followed by (d) a steep rise in voltage to a peak which occurs after (e) the current peak and during (f) the steep descent of current (as magnetic field energy is being consumed in ohmic heating), and finally, (g) a rapid decay of voltage after which damped oscillations of both current and voltage may or may not occur. The voltage peak occurs at about the times of the light flash and the transition of the wire boundary from linear to parabolic expansion with attendant shock wave generation.

The physical transformations of the wire, e.g. vaporization, expansion and establishment of arc discharge, corresponding to the distinguishable portions of the voltage, current and light output curves have been discussed by Müller[9] for the case of an explosion with a dark pause. The case without dark pause which matches our experimental data more closely has been considered in detail by David[10] both on the basis of Müller's experiments and from the theoretical point of view. He distinguishes stages which correspond to heating, melting, heating to bp, superheating of fluid metal, initial expansion, interruption of the current and further expansion of the metal vapor. It should be noted that the exploding wire experiments do not furnish positive experimental evidence for all of the features included by David, but that inferences from theory and from experiments made under equilibrium conditions play a considerable role in his discussion; nevertheless, the general correctness of the main outline of his argument can hardly be doubted, and it remains for further experimental work to verify or disprove the details of his model.

The voltage records of both Figures 6(a) and 6(b) show two easily interpreted features. The small break in the rising portion of the curve is evidence of melting of the wire. Keilhacker[11] in an experimental study of the vaporization of exploding wires and the equation of state for copper at high pressures and temperatures, presents current and voltage curves whose details are similar to ours. His examination of energy and resistance changes in the wire shows that the small, sudden rise in voltage corresponds to the rise in resistivity of copper on melting. The slope of the break apparently indicates that the melting does not take place everywhere at once. A large current is flowing and since the fundamental frequency is comparatively low, skin effect may be considered to be negligible. Current density is therefore practically uniform. This implies a large magnetic pressure of order 10^4 atm, on the wire axis, a pressure which falls parabolically to the external value (1 atm) at the surface. Thus melting must begin at the surface and progress inward as more energy is added and temperature raised.

The sharp rise in voltage after the break corresponds to a swift rise in resistance of the wire. There are two causes. The resistance rises rapidly because of ohmic heating and because the wire has begun to expand. David[10] estimates that for expansions between 2-5 diameters metallic conduction should cease. Measurements of Figure 6 show the diameter at voltage peak to be about three times the original value, and for this reason the wire should have ceased to conduct. What remains is conduction by thermionic emission modified by Schottky effect, but this mechanism is not able to sustain the large current flowing as is shown in the study of the current dwell and dark pause by Chace, et. al.[12]. Consequently current must start to fall, but as our Figure 6 shows does not fall very far. In the meantime voltage is falling also, thereby indicating a sharp decrease in resistance.

We infer and distinguish two types of electric conduction (arcs) to account for a fall in the voltage curve. The first is an ionized channel at or near the surface of the expanding wire. This arc is responsible for the sharp rise in light output and appears as the peripheral bright streaks in the rotating-mirror pictures. It corresponds to and is probably structurally identical with a continuum formed by the local air arcs postulated by Tucker[8].

The second electric discharge occurs along the axis of the wire at a sufficiently later time so that the density of metal vapor has dropped to a low value and a low-pressure metallic arc can strike.

The physical phenomena involved in these distinct types of arc formation are sufficiently complex and interesting to justify separate discussion of each type. As a by-product we arrive at a qualitative explanation of the current dwell that correlates well with much of the recently published data and provides considerable new insight into the sequence of events in a wire explosion.

3.3 The Peripheral Arc

This arc is caused mainly by the high voltage developed across the wire during the initial expansion of the wire. The sudden increase in resistance of the wire acts like a switch opening the circuit. When current starts to decrease, the collapse of magnetic field in the inductance of the entire circuit causes a large voltage of order 2-3 x 10^4 v to appear across the wire. This in itself is probably sufficient to cause breakdown of the air surrounding the wire, as may be seen by considering that our wires are 1.2 cm long and that the breakdown voltage for air at this electrode separation is 38 kv.

An additional contributing factor, electrical in nature, arises because of the radial motion of the wire boundary across the cylindrical magnetic field caused by the main current. In a paper on wires exploded in high vacuum, Kvartskhava *et. al.*[13] show the existence of a bright glow in a narrow annulus at the wire surface during early stages of the explosion. This is explained as a discharge caused by the main field along the wire plus the motional field, $\underline{v} \times \underline{B}$, experienced by particles moving radially with velocity $\underline{v}$ across the cylindrical magnetic field $\underline{B}$. In our first case the motional field is only about 5% ($\sim$ 1000 v/cm) of the peak field across the wire; but, on account of the hyperbolic field distribution outside the wire, is strongest right at the surface. Thus first breakdown of the medium should occur at or near the wire surface and shunting current density should be largest in a narrow cylindrical shell whose inner boundary is the expanding wire surface.

As the peripheral arc is formed, the large current flow transfers from the high-resistance wire interior to the low-resistance annular shell and both resistance and voltage drop to comparatively low values. As the wire expands the arc is pushed outward through the diminishing magnetic field and becomes less localized in space on account of diffusion and velocity spread of the constituents (cf. photographs given by Tucker[8]).

In the meantime the radiation excited by the peripheral arc decays and eventually disappears as energy in the circuit is expended. The type of radiation may be inferred from previous experiments on time-resolved spectra

from exploding wires in air[1,14]. There it is found that lines of nitrogen and oxygen appear at the beginning of the light flash and then decay rapidly, while the metal lines do not appear quite so soon but take several times as long to decay. This evidence supports the view that the peripheral arc initially excites radiation of the air adjacent to the wire and that the later appearing metal lines may be excited either by later stages of the peripheral arc or by the axial arc. While Kvartskhava et. al.[13] give no spectroscopic data on the glow they observe, one may infer that it represents a discharge set up in the permanent gases evolving from the metal surface under heating. A vacuum experiment on carefully degassed wires might show no glow at all.

3.4 The Axial Arc

In the event that the voltage maximum is too low to establish the peripheral arc, the phenomenon of dark pause or current dwell then ensues. Dark pause more commonly occurs with long wires (cf. Muller ref. 9); for which cases one infers the field strength to be too small to break down the medium at the wire surface. We have observed current dwell with our comparatively short wires, but only in explosions of larger than optimum wires where the voltage maximum occurs well after the current peak (see below § 3.6). In our cases the voltage peak is considerably below the value necessary for breakdown of the air. Current dwell has been observed by Webb et. al.[15] in 1 mil wires of length 0.29 in. While their wire length is only two-thirds ours, their ringing frequency of 6 mc is about twelve times greater. From their data one finds the field at voltage peak, including the motional field, to be about 30.3 kv/cm; whereas a value only 10% larger is needed for breakdown at their electrode separation[16]. Formative time lag for voltage breakdown of the air is probably an important factor in their experiments; for lacking a significant overvoltage a time lag of order 10 - 100 μsec may occur[17]. One may suppose then, that the primary cause of current dwell is failure of the peripheral arc to form, either because of insufficient field strength or because of insufficient overvoltage to counteract the formative time lag.

Once the dark pause occurs, arc formation of the axial type is the only remaining possibility. The Kerr cell schlieren pictures of Müller[9,18] show in a satisfactory way the development of dark pause, wire expansion and striking of the axial arc. Furthermore, the x-ray pictures of Thomer given in Müller's extended paper[18] show clearly the concentration of the dispersed metal into a cylindrical shell surrounding a less dense cylinder in whose interior the axial discharge takes place.

The details of formation of the axial arc are not well understood. These depend to considerable extent on the voltage remaining on the condenser at time of dark pause. If condenser voltage is comparatively high the arc may strike in the manner shown by Müller's data along what sometimes appears to be a helical interior path and, according to his explanation, presumably on the low-density side of the inward-facing, second shock as it approaches the axis.

This latter conclusion may be doubted for two reasons. First, Müller bases his supposition on numerical calculations made for the spherical blast wave by Wecken. These show a density minimum not at the axis but at the inner, low-density surface of the inward travelling second shock wave. Calculations made by Rouse[19] for the case of cylindrical symmetry and specifically for exploding copper wires in air do not show such a density minimum near the second shock, but rather nearly constant or slightly increasing density from the axis outward to the second shock. Second, some of our recent data[5] show in addition to peripheral arcs at the flash beginning, two types of axial arc, viz., (1) a streaked, expanding glow that starts within 1 μsec of the peripheral arc but within which the trajectory of the second shock may be faintly seen as it is carried outward in the interior flow and then returns, and (2) a bright, wedge-shaped glow which develops inside the trace of the second shock after it reflects from the axis and whose outer boundary seems to be limited by the inner surface of the dense cylindrical shell of expanded metal vapor.

Although direct proof is lacking, it seems obvious that the radiation excited by the axial arcs must consist mainly of metal lines. The slight delay between the peripheral and axial arcs would account for the already mentioned early appearance of air lines and the somewhat later appearance of metal lines. The greater duration and later intensity peak of the metal lines would correlate with the second form of axial arc which appears during reflection of the second shock from the axis.

3.5 Resistance, Power and Energy Curves

In Figures 7-11 we present data curves of current, voltage and light output, and calculated values of resistance, power and energy for 4 and 5 mil. Cu wires at several voltages. These data were obtained by measuring the oscilloscope records on a Telereader comparator, transferring the measurements onto punched cards and finally, calculating values of resistance, power and energy from $R = V/I$, $P_R = VI$, $E_R = \int_0^t P_R \, d\tau$ by means of routines programmed for the EDVAC computer. Calculated values can be immediately presented on punched cards so that the entire family of curves can be automatically plotted. This has been done in Figures 7-11. Voltage has been corrected for the inductive component of the exploding wire plus voltage divider circuit as described above in § 3.2.

The oscilloscope records of voltage and current are estimated from calibration data to be accurate to better than $\pm$ 2%; while the calibration accuracy with which the voltage and current shunts are known is better than 1%. The estimate for the current shunt refers to steady conditions of current measurement i.e. to continuous wave operation. A study of transient conditions at switch-on shows that the coaxial shunt will always report an initial slope of zero and therefore will underestimate the initial current ramp. This property of the shunt can cause considerable deviation of initial measured values from those predicted by RLC circuit theory; however the transient effects damp out to less than 3% in the first 1/8th cycle and at current peak are reduced to less than 0.2%.* On the other hand the

* Details of this work will be reported in a future paper.

inductive correction to voltage can decrease by perhaps as much as 15% as the wire expands. Thus correction of voltage using a constant inductance, as has been done here, can lead to errors as large as 400 v where current decline is largest. Voltage is always near peak value at this time so the possible error from this source is estimated at 5% or less. Combining these estimates we would expect maximum errors in current and voltage not to exceed 3% and 7% respectively and in the calculated quantities, not to exceed 10%. Exceptions can occur near a zero of the current, but elsewhere the upper bound of 10% is expected to hold.

An error, not accounted for in the preceding discussion, can arise from neglecting a voltage term I(dL/dt) caused by the change in dimensions of the conducting path as the wire expands. Insofar as it affects the calculated quantities, this term is largest near the current maximum during the linear expansion of the exploding wire. Estimates have been made for two possible situations,* viz., (1) uniform expansion of the 5 mil wire to 20 mil diameter in the time interval of the linear expansion of about 1/8 μsec, with current remaining constant, and (2) a change from 5 mil solid wire conduction to peripheral arc, sheath-conduction at 20 mil diameter in a time interval during the rapid rise in light intensity of about 1/16 μsec, with current at about two-thirds the maximum value. In neither case does the voltage from this term exceed 400 v. This voltage has the same magnitude and sign as the possible error due to overestimation of the L(dI/dt) correction made through the concomitant regime of current decrease. Thus the previous inductive correction, leaving inductance of wire and voltage divider constant, tends to compensate for neglect of the I(dL/dt) term. Accordingly, we make no correction for this term; yet expect the resulting voltage values to be within the 7% bound on error.

---

* As Keilhacker[11] points out, during the initial expansion the conductivity of outer layers of the wire will decrease and current will concentrate toward the center. Such an effect would diminish the inductance change in (1) or might in extreme cases change its sign.

3.6 Energy Deposit in the Wire

Comparison of the energy curves in Figures 7-11 with each other, with the power curves and with the correlated streak and oscilloscope data of Figure 7 shows some interesting facts. We note the following: (a) comparatively little energy ($\sim$ 1 joule) is deposited in the wire before the current peak is reached, (b) after current peak, energy is deposited rapidly according to a steeply rising function during an interval of 0.2 - 0.3 μsec, (c) at the end of this interval the energy curve levels off on a plateau at nearly constant value, (d) the current curve decreases during the deposition of energy, most rapidly where the rate of energy addition is largest, (e) where current does not fall to comparatively small values ($\leq$ 2 kiloamp) small additional amounts of energy are added over a much longer period, $\sim$ 0.5 μsec, during the phase which may be identified by both the increase in light output and the low resistance values as peripheral-arc conduction, and finally (f) at the elbow or plateau of the energy curve, the energy deposited lies between 40% and 60% of the total stored in the capacitors and amounts in the best case to about 12 ev per atom.

The 5 mil wire at 10.8 kv, Figure 10, provides an especially interesting example; for in this case the current value drops to zero, energy deposited remains constant and a small negative voltage, ca. 1 kv, remains on the condenser. Despite the fact that this condition resembles the onset of dwell, further experiments with longer sweep times show that the condenser voltage gradually returns to zero, presumably by leakage, with no further oscillation of current. A streak interferogram for this case[20] shows that after the peripheral-arc phase no further light output occurs. It is thus made clear that insufficient energy remains on the condenser to cause the axial arcs which illuminate the second shock wave observed in other cases, e.g. 4 mil wire at 9.2 - 12.8 kv. One may also infer that the second shock wave, seen in these examples as a wedge-shaped luminosity occurring several μsec after the peripheral arc, may not usually be luminous of itself, but derives luminosity from the arc discharge which occurs behind the shock in the region of increased temperature, ionization and conductivity.

When one considers the important effect of the peripheral arc on the resistance offered by the wire and parallel conduction paths, a qualitative explanation of the strong dependence of shock wave energy on ambient air density reported in an earlier paper[21] now seems possible. Evidence is given there that reducing ambient air pressure to values as low as 1/8 atm reduces the apparent energy of the head shock wave by a factor of six or more. Considering the Paschen curve for air we note that reduced ambient pressure will allow the peripheral arc to occur at a proportionately lower voltage. As a consequence the wire and path resistance falls at slightly earlier times than formerly and may not pass through the most favorable range of values as current reaches its maximum value. The result would be that smaller amounts of energy are absorbed by the wire and the energy transfer to flow phenomena in the ambient medium would be thereby reduced.

The question of optimum wire resistance for maximum energy transfer has been discussed in our previous papers[2,22]. The estimate is given there that the mean resistance value for the entire circuit during an interval including the current peak should lie somewhere in the range $1.1 \leq R_{opt}\left[\frac{C}{L}\right]^{-1/2} \leq 1.3$. With the present circuit constants (cf. § 2.3) this inequality indicates a value in the range $0.80 \leq R \leq 0.95$. Since the circuit resistance exclusive of exploding wire is about 0.15 ohm, the wire ought to furnish about 0.65 - 0.80 ohms. Now the peak resistance values shown in Figures 7-11 exceed 2.8 ohms; however mean values calculated from resistance weighted by current squared i.e. $\bar{R} = \int_0^{t_1} RI^2 dt \left[\int_0^{t_1} I^2 dt\right]^{-1}$, (with t_1 taken at the plateau of energy) show the 4 mil wires to have mean resistances in the range 0.78 - 1.20 ohms and the 5 mil wires in the range 0.44 - 0.63 ohms. Empirically the 5 mil wires seem to be slightly the better match and their mean values do not quite overlap the lower end of the range of predicted values while the 4 mil wires just overlap from above.

We may conclude from this analysis of data that the inequality for mean resistance has a certain somewhat limited validity when mean resistance is calculated using the ratio of integrated resistive power to integrated

squared current. The inequality may be viewed as a rule of thumb helpful in selecting wires that may be in the neighborhood of optimum match. On the other hand the theory on which the inequality is based takes no account of resistance change during the early expansion, relies on prior estimates of the order of magnitude of resistance increase, and leaves out of consideration the interrelation of the expanding wire and the motion of the surrounding medium.

E. David[23] has given a different criterion for maximum heating of an exploding wire. According to his theory a factor Q should be approximately 1.2 where Q is essentially the ratio of mean resistance to circuit matching resistance (defined in his paper as $\left[L/C\right]^{1/2}$) multiplied by the ratio of stored condenser energy to energy necessary to heat the wire to 5000°C. Since this latter ratio is easily made 30 or more, David's criterion predicts that average wire resistance should be smaller than the circuit matching resistance by a factor equal to the reciprocal of this ratio. This is one or two orders of magnitude smaller than the values suggested by our inequality and calculated from our experimental data.

David's theoretical model while including in an approximate way the effects of heating the wire, ignores the important influence of resistance in maximizing both resistive power consumption and energy transfer from magnetic field storage to ohmic heating and fluid motions. It may be doubted whether his criterion has any application in situations where maximum energy transfer is necessary to achieve maximum heating.

We close this section by discussing briefly the behaviour of wires incapable of matching the circuit even approximately. Figures 12 and 13 show some typical current and voltage records for wires too small (3 mil) and too large (5.5 - 6.3 mil) to match the circuit. The small wires clearly are heated too rapidly and start to expand during the current rise. As the expansion proceeds the wire resistance rises abruptly, current dips momentarily while voltage rises steeply until a peripheral arc forms. Resistance then falls and current resumes its increasing trend. Axial arcs can form after the

wire has expanded slightly more and the circuit sustains damped oscillations with energy dissipated internally and in the arcs. Many of the examples given in the literature are of this type. See for example Reithel et. al.[1] and probably Scherrer[24]. The latter author supposes that matching between wire and circuit can occur during the later expansion phase when wire resistance is falling. Our data does not support this belief and in the absence of clear supporting evidence we must regard his assumption as unfounded.

The larger wires show variations of dark pause behaviour depending on voltage. The 5.5 mil wire at 12.4 kv is typical of previously reported dwell-time observations[9,25] save possibly for the reversal of voltage and current. In contrast, our 5.5 - 6.3 mil wires at lower voltages show development of a dwell phenomenon in the second and third half-cycles of the current. Here a small voltage (resistance) rise is noticeable in the first cycle but is evidently insufficient to absorb enough energy to expand the wire until one or two more half cycles occur. The larger wires at low voltages produce very little light and in some cases appear more like a shower of sparks than a concentrated light source. One may suppose that the wire is melting, forming unduloids and then pinching off, leaving a series of molten droplets and connecting arcs. Events of this kind are reported by Zernow et. al.[26].

3.7 The Shock Waves

Measurements of shock wave trajectories out to about 6 μsec have been made from the streak pictures of wires corresponding to Figures 7-11. Beyond 6 μsec the wave may no longer be considered even approximately a strong shock in the sense of similarity theory, and in addition, deviations from cylindrical symmetry caused by disturbances reflected from the wire holders are probably no longer negligible.

Two types of analysis have been applied to this data. First, axial energy E in joules/cm released to the shock wave is determined according to our usual procedure[2,21] from the similarity theory for a strong cylindrical

shock wave given by S. C. Lin[27] and compared to values determined from Sakurai's[28] second approximation to the first order theory. This comparison allows some tentative conclusions regarding the improvement to be expected in values of E if the Sakurai equation is used. Secondly, through a connection provided by the similarity flow theory for shocks with energy release variable with time, we compare the power law characterizing the early development of the shock wave with the power law describing the electrical energy as a function of time. From this comparison we draw preliminary conclusions regarding a question proposed in an earlier paper[21], viz., whether the power law of energy deposition in the wire controls the power law of shock wave growth during its earliest phase.

The shock trajectory to the second approximation of Sakurai can be expressed as $Y = (2R)^2 - .00932\ t^2 = 366.28\ (E/p_o)^{1/2} t$ where R is shock radius in cm, t is time in sec, E is joules/cm axial energy release at $t = o$, and p_o is ambient pressure in dynes/cm^2 for a gas of $\gamma = 1.4$. If the coefficient of t^2 is set equal to zero and use is made of the relation $p_o = c^2 \rho_o/\gamma$ (with c = 340 m/sec.) the above equation reduces to the first order form of Lin.

Shock data corresponding to the 4 and 5 mil wires of Figures 7-11 have been fitted to both the Lin and Sakurai equations by plotting Y vs t and selecting the best straight line graphically. E values from the Lin (Sakurai) formula for the five cases, in the same order as Figures 7-11, are 9.1 (8.4), 12.2 (12.7), 15.2 (14.5), 9.4 (9.4), and 14.6 (14.7) joules per cm respectively. It will be seen that electrical energy deposited in the wire* at the upper elbow of the curve (i.e. by the time of greatest curvature) is 0 - 15% less than the energy of the shock wave for the 4 mil wire cases, whereas it exceeds by 10 - 30% the energy of the shock for the 5 mil cases. This tends to confirm the fact previously found[2] that the 4 mil wire is more efficient in transfer of energy from electrical to mechanical form than any other tested.

---

* N.B. The value of E_R read off the curve must be divided by 1.2 , the length of the wire, to obtain the appropriate joules/cm value for comparison.

Because the quadratic term has a negative sign, the Sakurai plot will always lie below the Lin plot and consequently should always give smaller values of E. In our cases the correction to the $(2R)^2$ term was never more than 4% at the largest times used and the variability of slope encountered by the graphical fitting technique is greater than the consistent lowering produced by the quadratic correction term. It is sometimes easier to choose a linear fit to the Sakurai plot, but the calculation takes longer; so if energy values consistent only to about 5% are desired, the advantage would seem to lie with the Lin equation. For higher energies than these, the difference between the two methods diminishes. For lower values it becomes increasingly more important. Below values of 5 joules/cm one should probably prefer the Sakurai plot.

Whether the shock trajectory data is plotted according to the Lin or to the Sakurai approximation, the resulting curve is noticeably concave upward during the first microsecond interval and slightly concave upward thereafter. In a previous paper[21] it is shown that, for certain examples, plots of $(2R)^n$ vs t with $n \doteq 5/3$ eliminate the early curved portion of the trajectory for times less than 1 μsec and straighten the plot at later times. There it is pointed out that according to the general theory, similarity solutions may be obtained when axial energy release to the flow is given by a power law of time with the exponent $(4/n) - 2$. When $n = 2$ energy addition is independent of time and the Lin shock trajectory is obtained. All non-zero values of n imply both variable energy release with time and curved trajectories on a parabola test plot of $(2R)^2$ vs t.

In order to determine whether the general similarity theory is capable of representing the relationship between deposit of electrical energy and the power law of the shock trajectory, the energy data of Figures 7-11 have been subjected to the following analysis. From logarithmic plots of energy vs time the best straight line fit has been chosen for each example and a power m determined such that $E \propto t^m$. In most cases the fit to the experimental points is very good except for energies less than one joule.

By logarithmic plotting followed by a graphical check of form $(2R)^n$ vs t, values of n were determined for each shock trajectory. The validity of relation $m = (4/n) - 2$ could then be checked by substitution. The result is negative.

The m values lie in the range $2.6 \leq m \leq 3.2$, while the n values satisfy $1.35 \leq n \leq 1.65$ which inequality implies values for m in the interval 0.4 - 1.0. The agreement is not even approximate. The conclusion may be drawn that for the present cases the shock trajectory and law of energy deposit are not related by similarity flow theory. In view of the many deviations of the experimental situation from those under which the similarity theory would be strictly applicable, the failure of this test may occasion no suprise, but it is all the more remarkable that the shock trajectory should follow a similarity-law trajectory over a considerable portion of its range and that energy values derived from the similarity theory should be consistent with independent electrical measurements.[2]

F. D. Bennett

F. D. BENNETT

H. S. Burden

H. S. BURDEN

D. D. Shear

D. D. SHEAR

REFERENCES

1. Reithel, Blackburn, Seay and Skolnick, Exploding Wires, W. G. Chace and H. K. Moore, Eds. (Plenum Press, Inc., New York 1959) p. 19. Future references to this book will be indicated by EW followed by page number.

2. Bennett, F. D., Phys. Fluids 1, 515, (1958).

3. Brauer, F. L. and Hansen, D. F., J. Opt. Soc. Am. 49, 421 (1959).

4. Courtney-Pratt, J. S., Reports on Progress in Physics, Vol. 20 (The Physical Society, London 1957) p. 384.

5. Bennett, F. D., Shear, D. D. and Burden, H. S., Streak Interferometry, BRL Report 1080, (Aberdeen Proving Ground, Maryland, 1959) pp 20-21. See also J. Opt. Soc. Am. 50, 212 (1960) although Figure 3 of this reference was retouched by the publishers and the wire shadow eliminated.

6. Park, J. H., J. Research Natl. Bur. Standards 39, 191 (1947).

7. Bennett, F. D., Cylindrical Shock Waves from Exploded Wires of Hydrogen-Charged Palladium, BRL Report 1063 (Jan 1959) See Figures 1(e) and 1(f).

8. Tucker, T. J., J. Appl. Phys. 30, 1841 (1959).

9. Müller, W., Z. Physik 149, 397 (1957).

10. David, E., Z. Physik 150, 162 (1958).

11. Keilhacker, M., Z. angew. Physik 12, 49 (1960).

12. Chace, W. G., Morgan, R. L. and Saari, K. R., EW, p 59.

13. Kvartskhava, Bondarenko, Meladze and Suladze, Soviet Phys. JEPT 4, 637 (1957).

14. Lewis, M. R. and Sleator, D. B., Exploding Wire Light Source for High Speed Interferometry, BRLM 975 (BRL, Aberdeen Proving Ground, Maryland, 1956) p 29.

15. Webb, F. H., Jr., Bingham, H. H. and Tollestrup, A. V., Phys. of Fluids 3, 318 (1960).

16. AIP Physics Handbook Section 5, p. 179.

17. ibid. p. 180.

REFERENCES (cont'd)

18. Müller, W., EW, p. 186.

19. Rouse, C. A., EW, p. 227.

20. Bennett, Burden and Shear, J. Opt. Soc. Am. 50, 212 (1960), cf. Figure 2 (d).

21. Bennett, F. D., EW, p. 211.

22. Bennett, F. D., BRL Report No. 1056 (Oct 1958) cf. Appendix I.

23. David, E., EW, p. 271.

24. Scherrer, V. E., EW, p. 118.

25. Fünfer, Keilhacker and Lehner, Z. angew. Physik 10, 157 (1958).

26. Zernow, Woffinden and Kreyenhagen, Phot. Sci. and Eng. 4, 31 (1960).

27. Lin, S. C., J. Appl. Phys. 25, 54, (1954).

28. Sakurai, A., EW, p. 264.

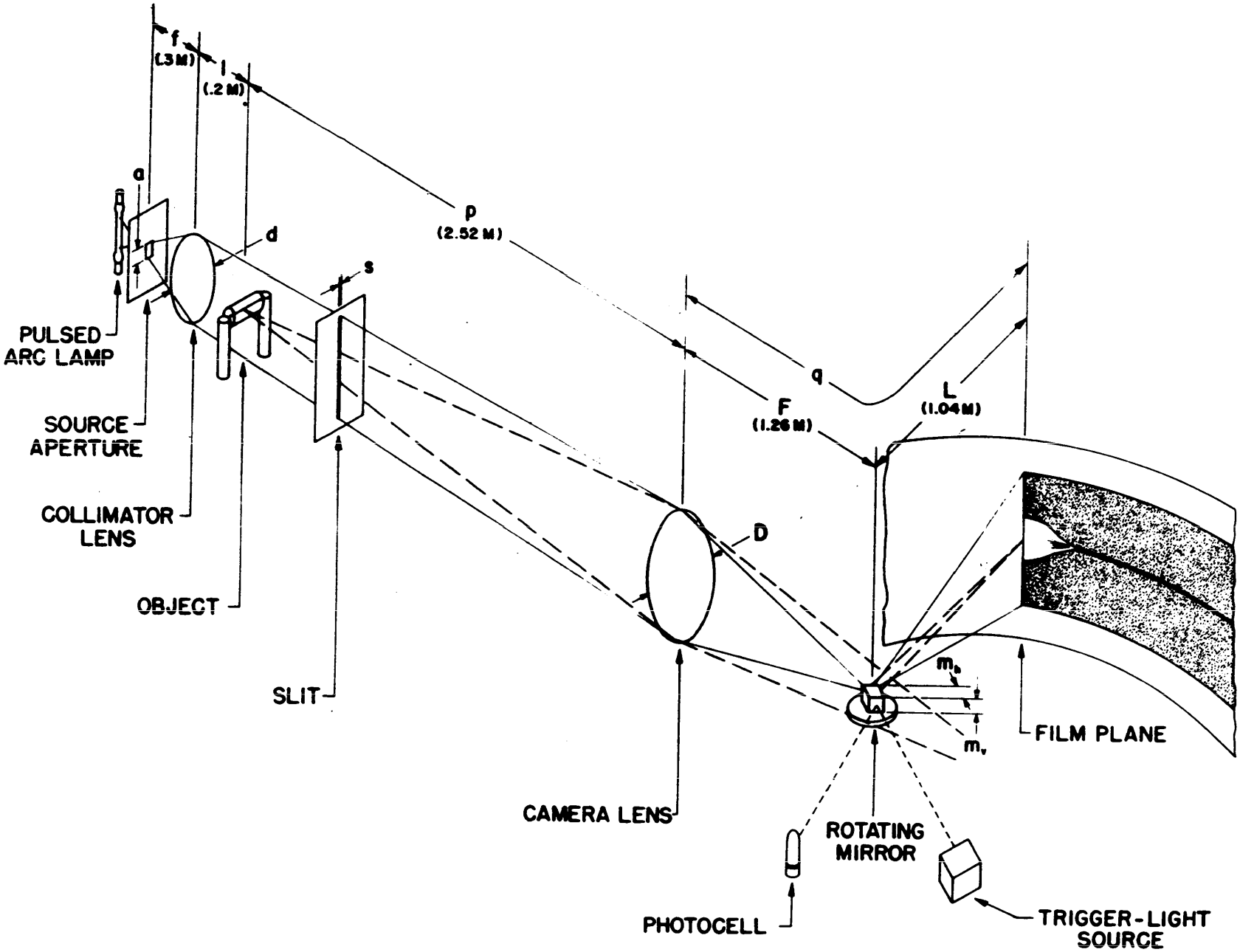

FIGURE 1. Schematic Diagram of Rotating Mirror Camera

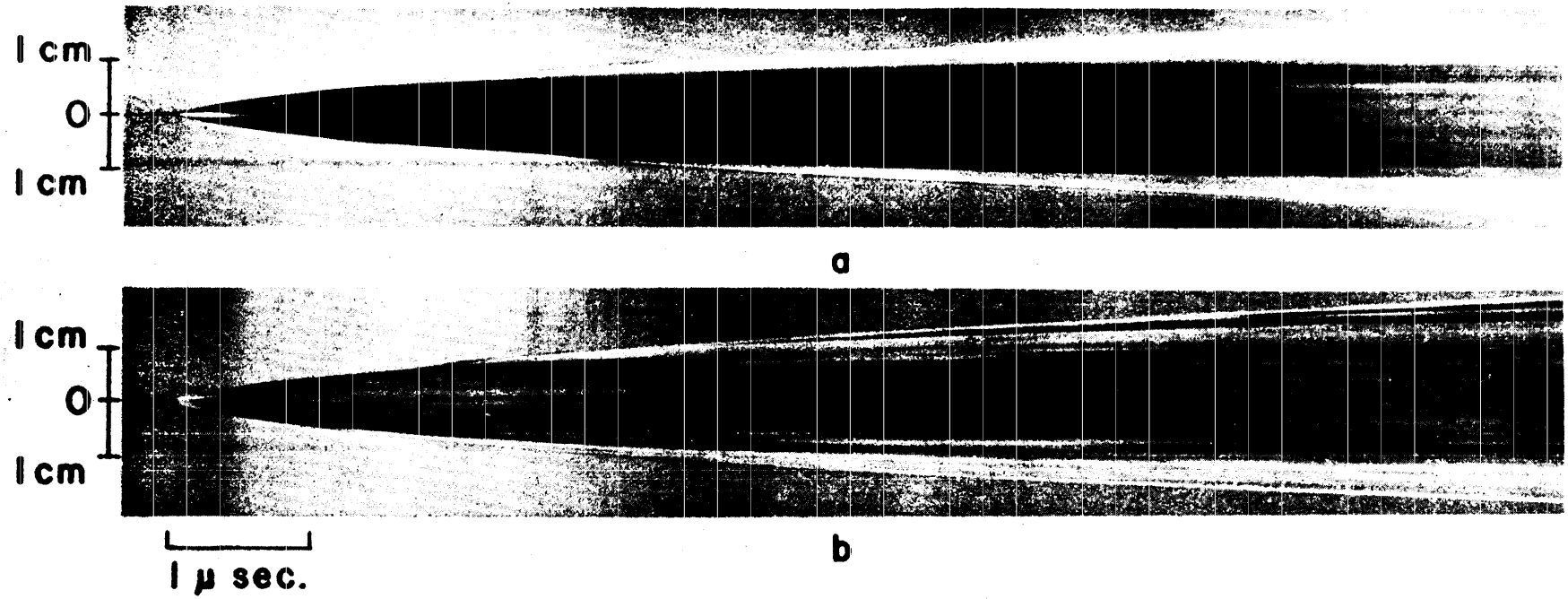

FIGURE 2. (a) 4 mil Cu wire at 9.2 kv
(b) 4 mil Cu wire at 12.4 kv

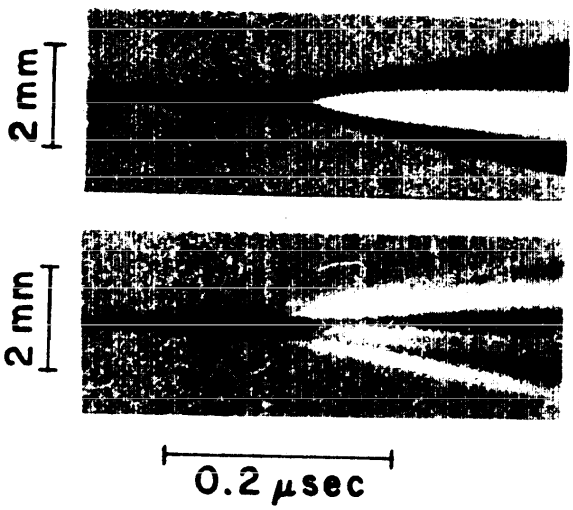

FIGURE 2. (c) Enlargement of tip region

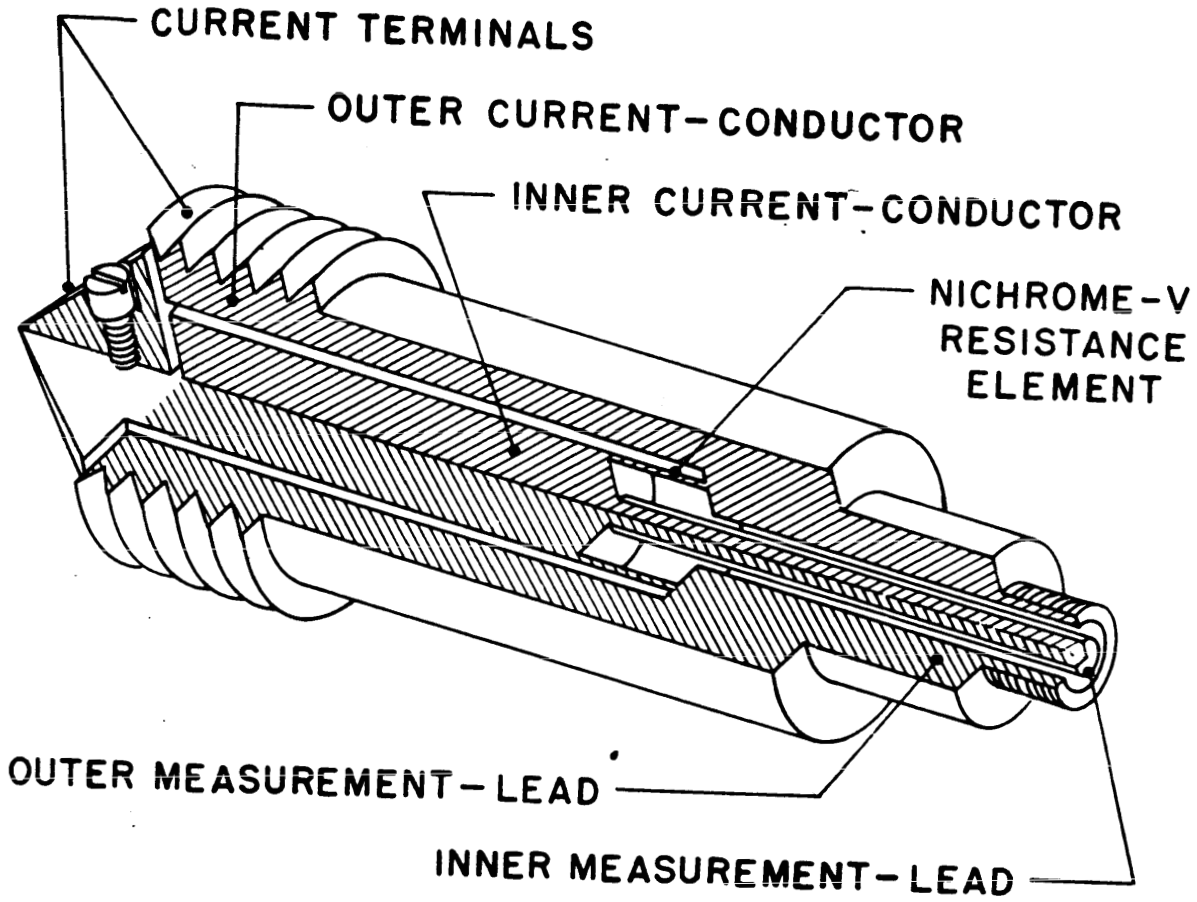

FIGURE 3. Schematic of Current Shunt (5 times normal size)

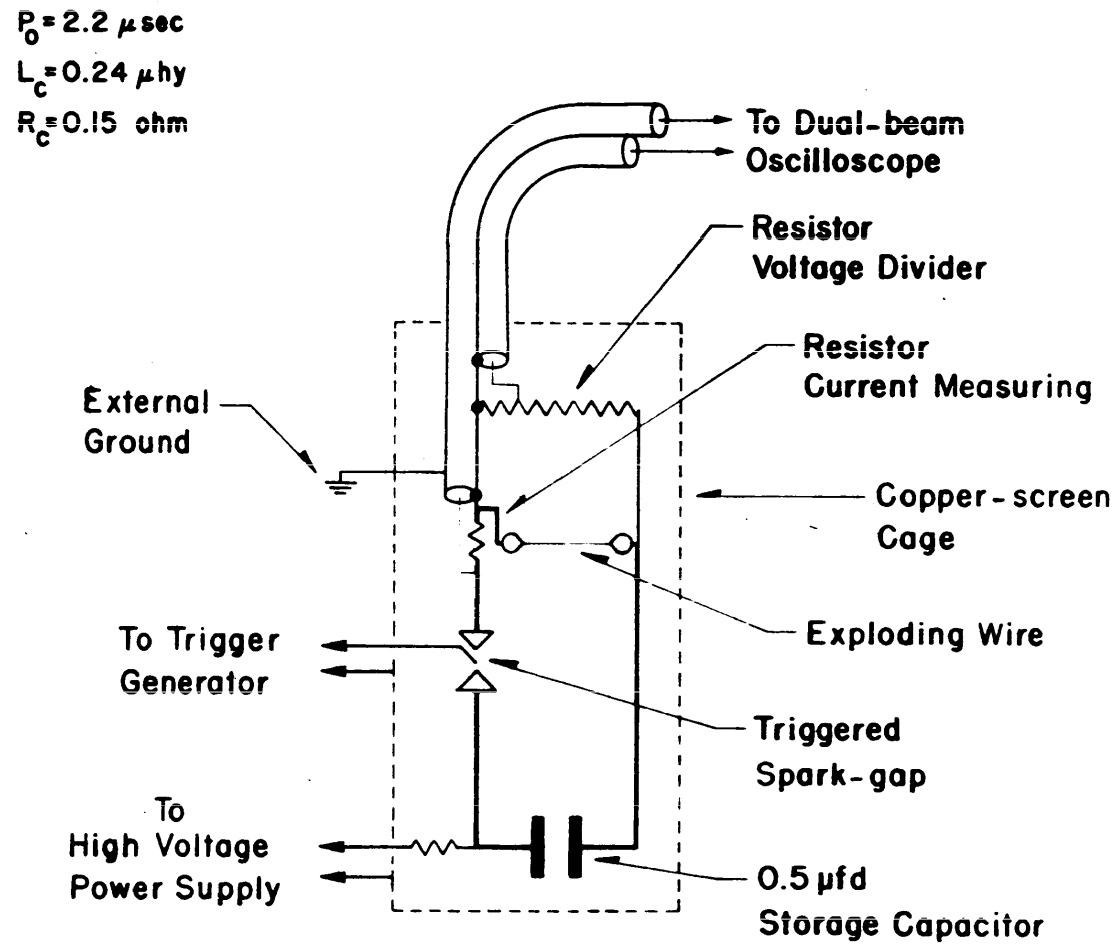

FIGURE 4. Exploding Wire Circuit Showing Shunt and Voltage Divider

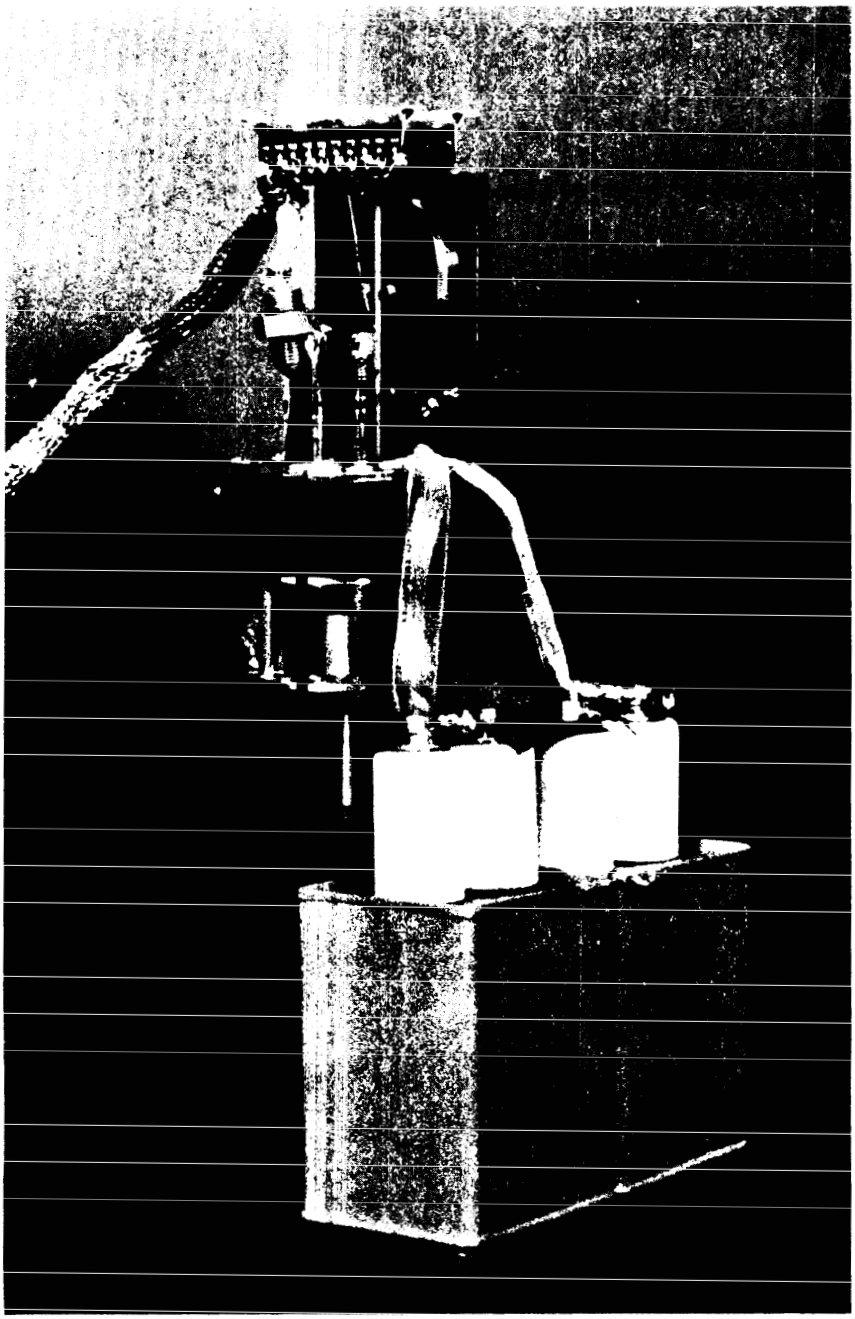

FIGURE 5. View of Experimental Exploding Wire Equipment

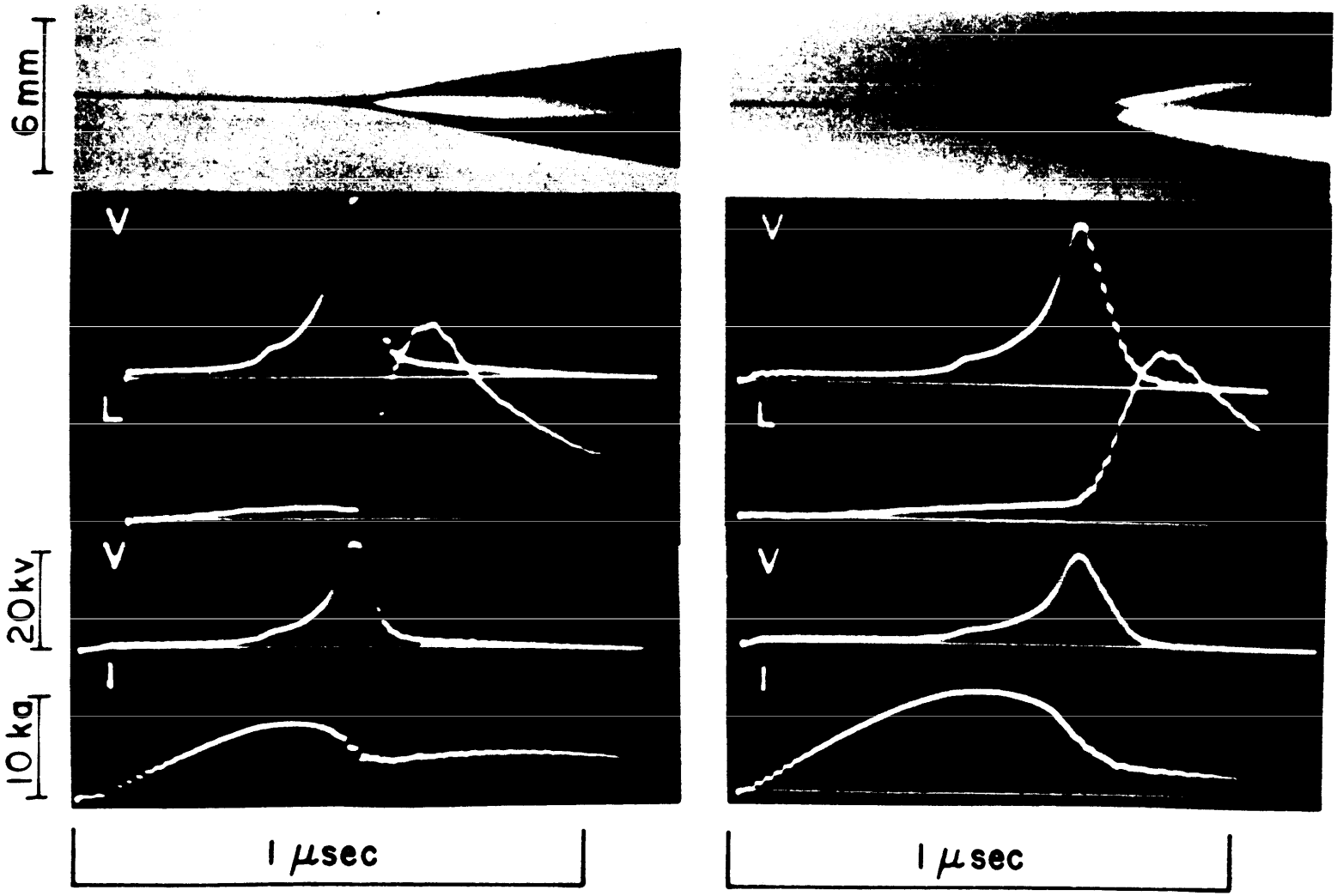

FIGURE 6. (a) Composite Optical and Electrical Data for 1.2 cm, 4 mil Cu wire at 9.2 kv I - current, V - voltage, L - light
(b) Composite data for 1.2 cm, 5 mil Cu wire at 12.4 kv

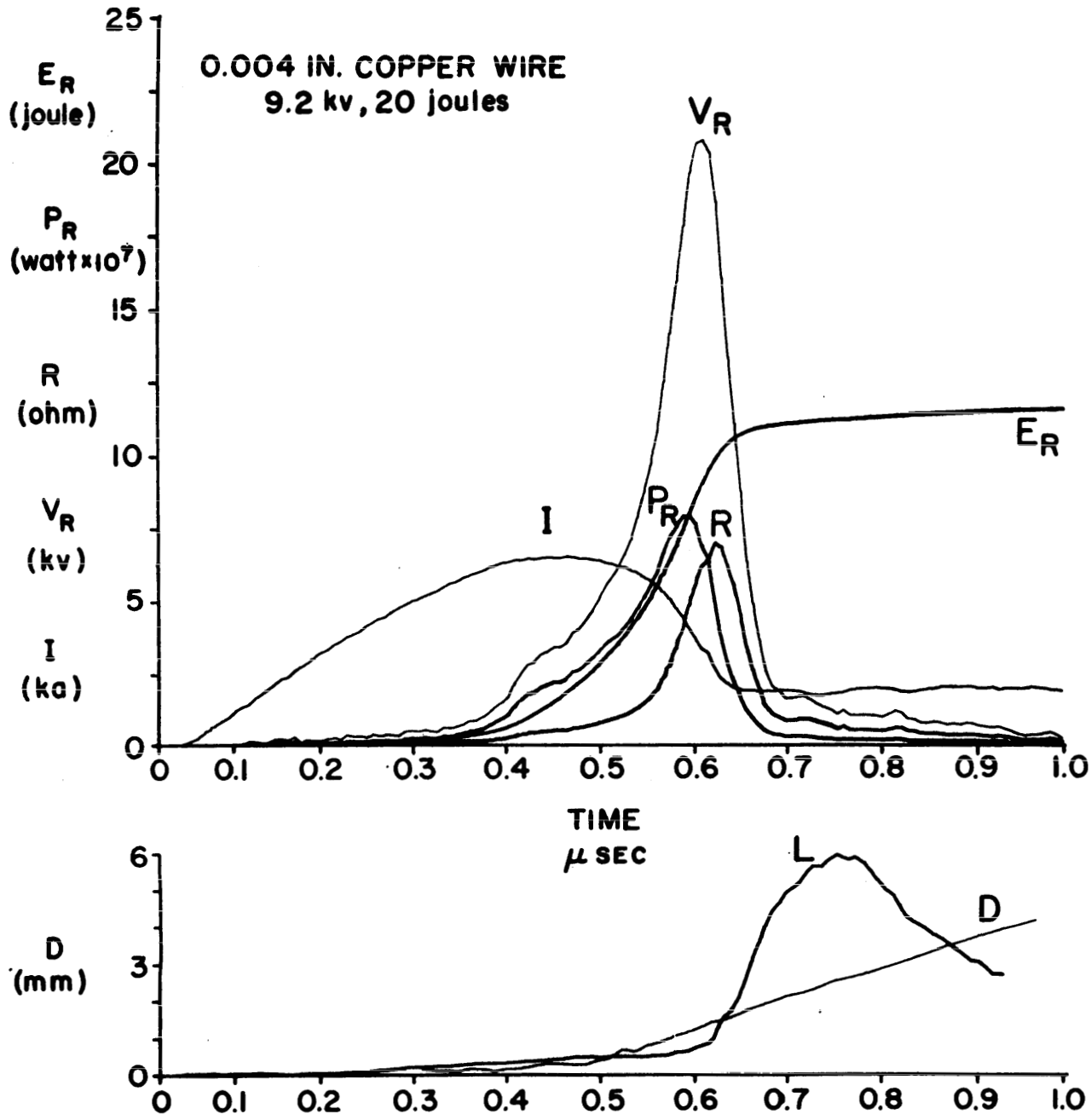

FIGURE 7. 4 mil Cu at 9.2 kv I - current, R - resistance, V_R - resistive voltage, P_R - resistive power, E_R - energy, L - light output, D - wire diameter

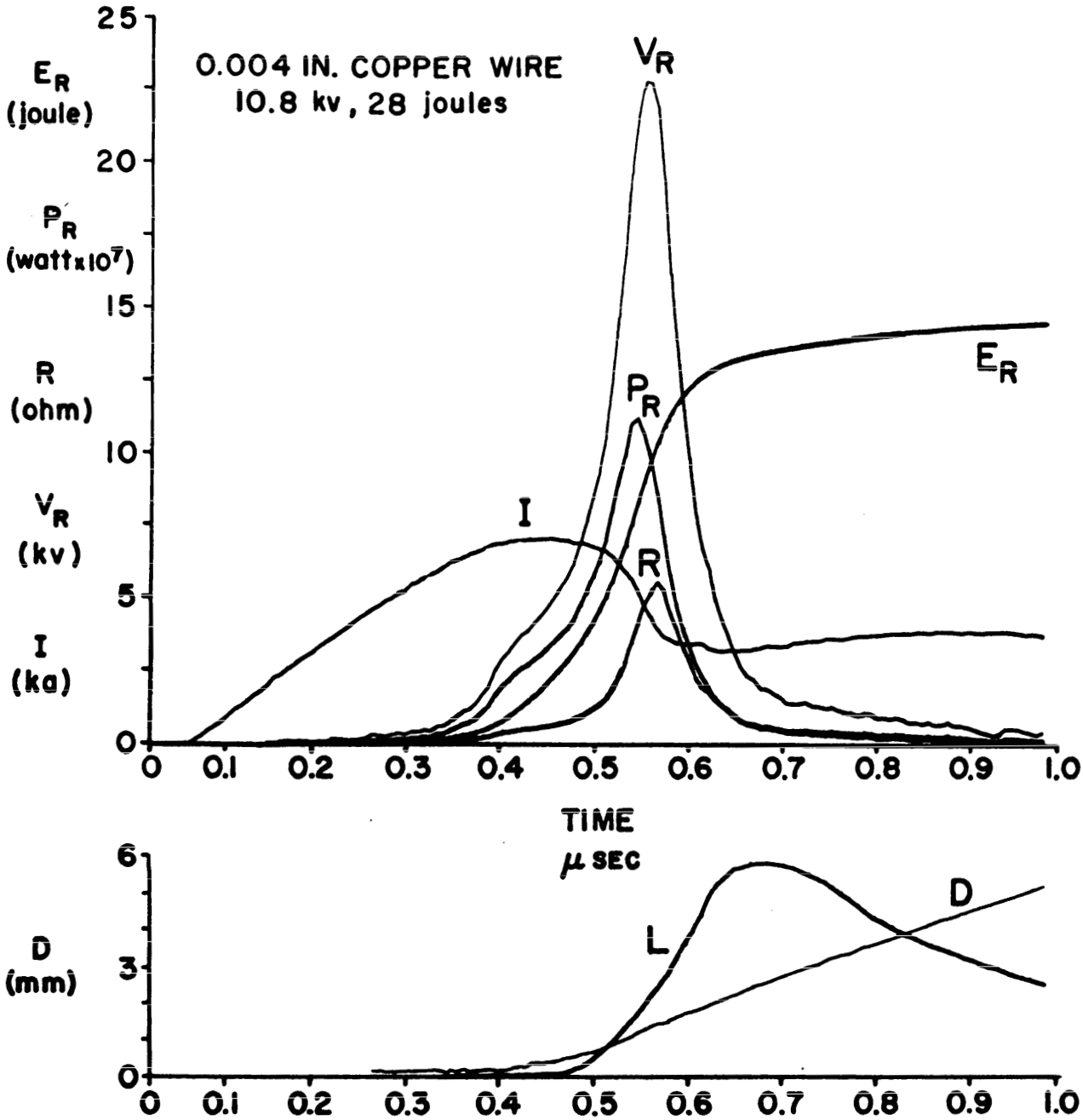

FIGURE 8. 4 mil Cu at 10.8 kv

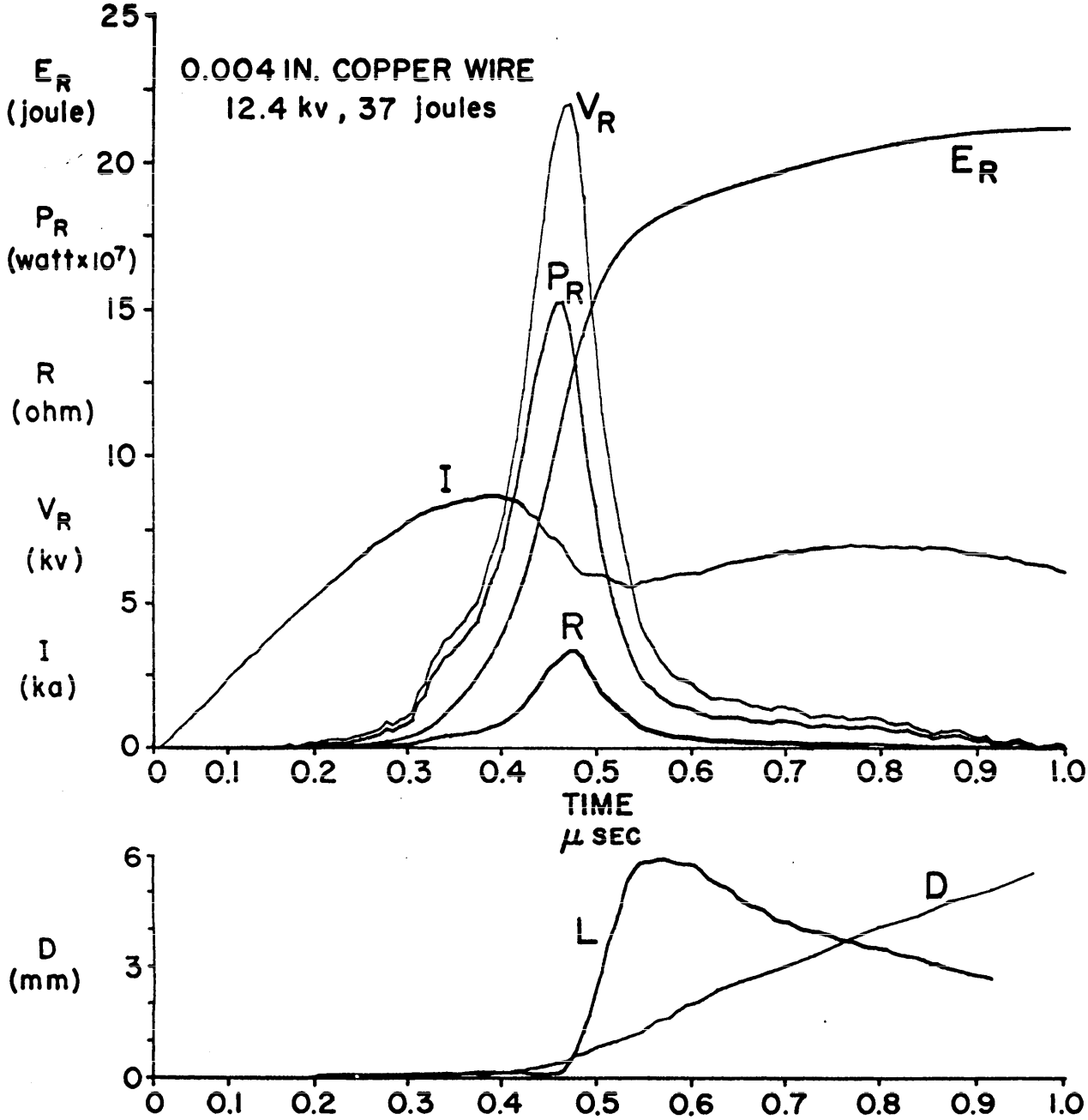

FIGURE 9. 4 mil Cu at 12.4 kv

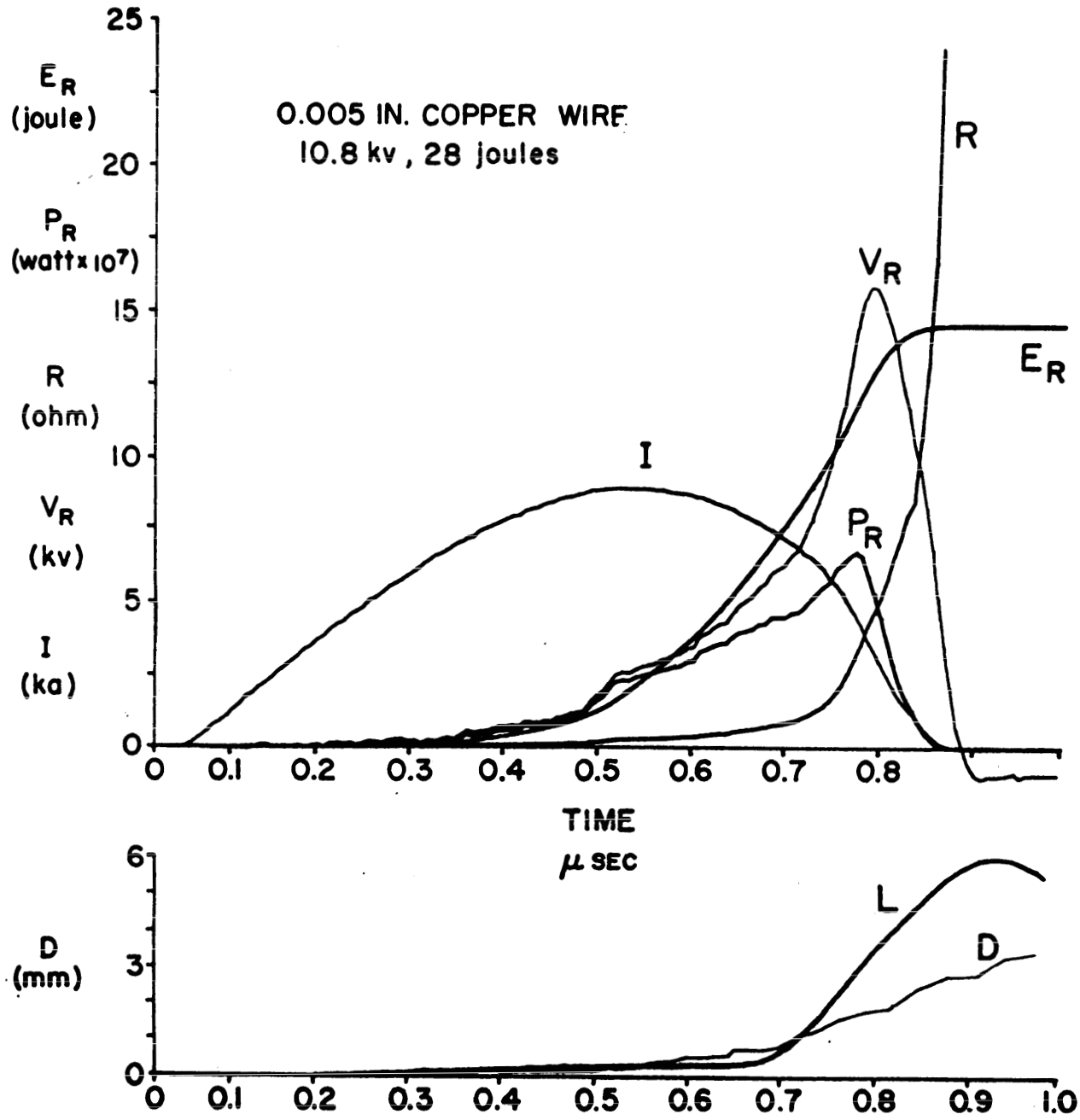

FIGURE 10. 5 mil Cu at 10.8 kv

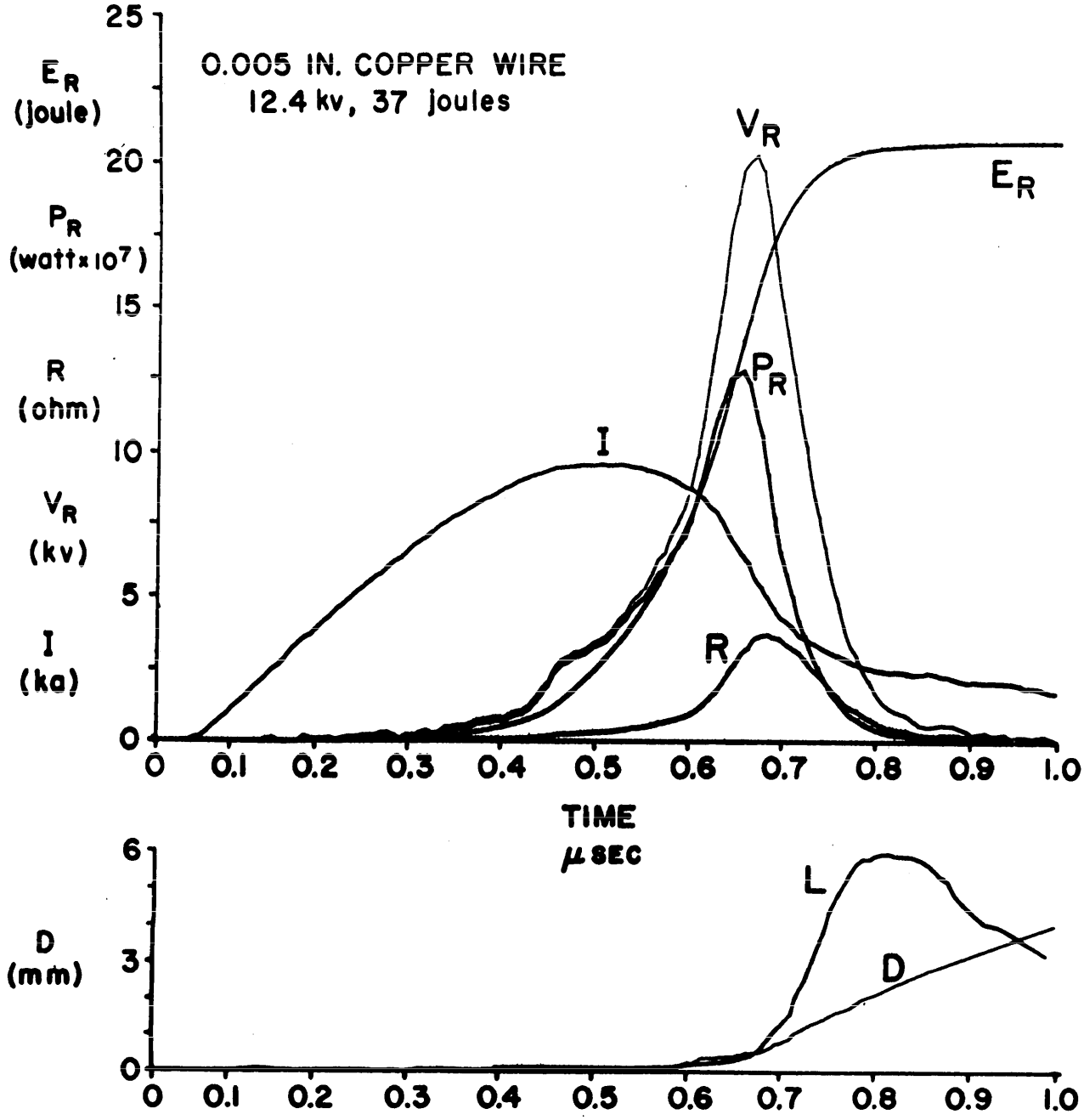

FIGURE 11. 5 mil Cu at 12.4 kv

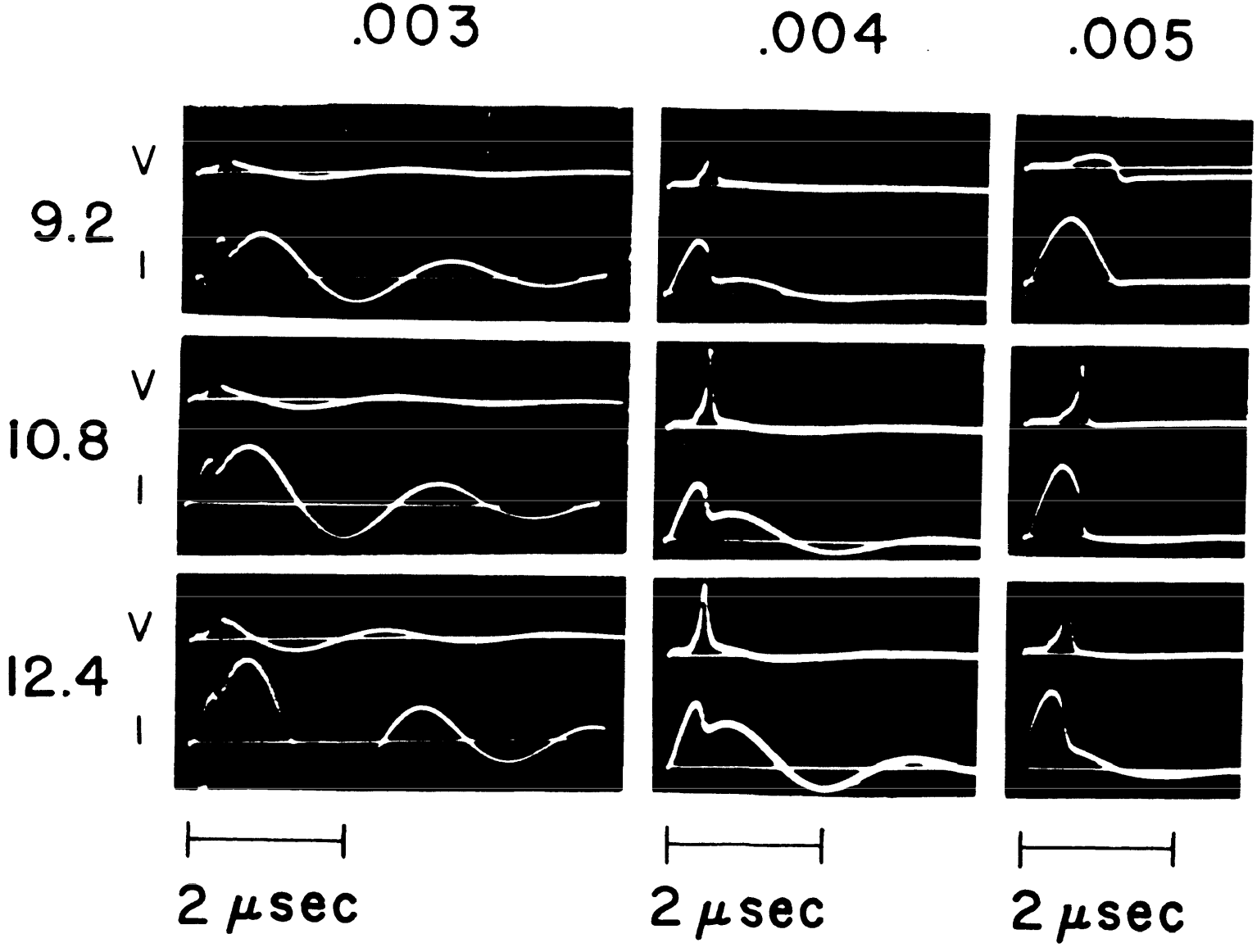

FIGURE 12. Voltage and Current Curves for 3, 4, and 5 mil Wires

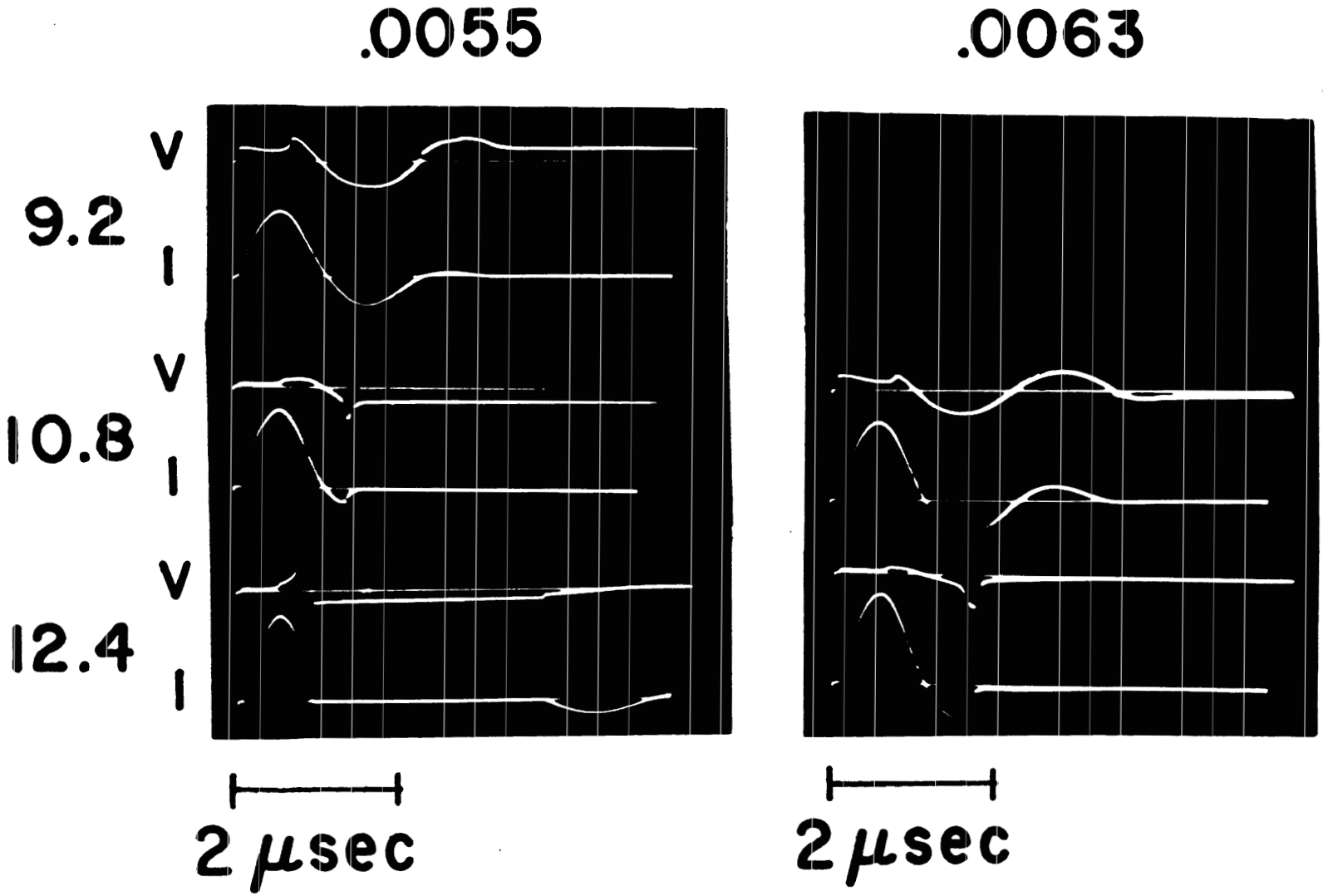

FIGURE 13. Voltage and Current Curves for 5.5 and 6.3 mil Wires

DISTRIBUTION LIST

No. of Copies	Organization
2	Chief of Ordnance ATTN: ORDTB - Bal Sec ORDTN Department of the Army Washington 25, D. C.
1	Commanding Officer Diamond Ordnance Fuze Laboratories ATTN: Technical Information Office Branch 012 Washington 25, D. C.
10	Commander Armed Services Technical Information Agency ATTN: TIPCR Arlington Hall Station Arlington 12, Virginia
10	Commander British Army Staff British Defence Staff (W) ATTN: Reports Officer 3100 Massachusetts Avenue, N.W. Washington 8, D. C.
4	Defence Research Member Canadian Joint Staff 2450 Massachusetts Avenue, N.W. Washington 8, D. C.
3	Chief, Bureau of Naval Weapons ATTN: DIS-33 Department of the Navy Washington 25, D. C.
1	Commander Naval Ordnance Laboratory ATTN: Library White Oak, Silver Spring 19 Maryland
1	Commander U. S. Naval Ordnance Test Station ATTN: Technical Library China Lake, California
1	Superintendent U. S. Naval Postgraduate School Monterey, California
1	Director U. S. Naval Research Laboratory ATTN: Dr. A. C. Kolb Washington 25, D. C.
1	Commander U. S. Naval Weapons Laboratory Dahlgren, Virginia
1	Commander Air Proving Ground Center ATTN: PGEM Eglin Air Force Base, Florida
3	Commander Air Force Cambridge Research Laboratory ATTN: W. G. Chace - CRZN M. A. Levine M. O'Day L. G. Hanscom Field Bedford, Massachusetts
1	Commander Air Force Special Weapons Center ATTN: SWRP Kirtland Air Force Base New Mexico
1	Director Air University Library ATTN: AUL (3T-AUL-60-118) Maxwell Air Force Base, Alabama

DISTRIBUTION LIST

No. of Copies	Organization
1	Commander Aeronautical Systems Division ATTN: WWAD Wright-Patterson Air Force Base Ohio
2	Commanding General Frankford Arsenal ATTN: Mr. Charles Lukens Bldg. 150 Library Branch, 0270 Bldg. 40 Philadelphia 37, Pennsylvania
3	Commanding Officer Picatinny Arsenal ATTN: Feltman Research and Engineering Laboratories NASL Mr. S. S. Verner Dover, New Jersey
1	Commanding General Army Ballistic Missile Agency ATTN: Dr. T. A. Barr Redstone Arsenal, Alabama
1	Commanding General Army Rocket & Guided Missile Agency ATTN: Supporting Research Branch Redstone Arsenal, Alabama
1	Army Research Office Arlington Hall Station Arlington, Virginia
1	Applied Physics Laboratory The Johns Hopkins University 8621 Georgia Avenue Silver Spring, Maryland
1	Jet Propulsion Laboratory ATTN: Mr. Irl E. Newlan Reports Group 4800 Oak Grove Drive Pasadena, California
1	Director National Aeronautics & Space Administration 1520 H Street, N.W. Washington 25, D. C.
2	Director National Aeronautics & Space Administration Ames Research Center ATTN: Mr. V. J. Stevens Mr. Harvey Allen Moffett Field, California
1	Director National Aeronautics & Space Administration Langley Research Center Langley Field, Virginia
1	Director National Aeronautics & Space Administration Lewis Research Center Cleveland Airport Cleveland, Ohio
1	Director National Bureau of Standards ATTN: Mr. Paul H. Krupenie 232 Dynamometer Building Washington 25, D. C.
1	U. S. Atomic Energy Commission ATTN: Technical Reports Library Mrs. J. O'Leary for Division of Military Applications Washington 25, D. C.
3	U. S. Atomic Energy Commission Los Alamos Scientific Laboratory ATTN: Dr. J. L. Tuck Dr. R. G. Schreffler Dr. R. E. Duff P. O. Box 1663 Los Alamos, New Mexico

DISTRIBUTION LIST

No. of Copies	Organization
1	Cornell Aeronautical Laboratory, Inc. ATTN: Mr. Joseph Desmond Librarian 4455 Genessee Street Buffalo 5, New York
1	Datamatic Corporation ATTN: Dr. R. F. Clippinger 151 Needham Street Newton Highlands 61, Massachusetts
2	General Electric Research Laboratory ATTN: Dr. R. A. Alpher Dr. D. R. White P. O. Box 1088 Schenectady, New York
1	California Institute of Technology Aeronautics Department ATTN: Professor H. W. Liepmann 1201 East California Street Pasadena 4, California
1	California Institute of Technology Guggenheim Aeronautical Laboratory ATTN: Professor L. Lees Pasadena 4, California
1	Case Institute of Technology Department of Mechanical Engineering ATTN: Professor G. Kuerti University Circle Cleveland 6, Ohio
1	Cornell University Graduate School of Aeronautical Engineering ATTN: Professor E. L. Resler Ithaca, New York
1	Harvard Observatory Harvard University ATTN: Professor F. L. Whipple Cambridge 38, Massachusetts
1	The Johns Hopkins University Department of Aeronautics ATTN: Professor L.S.G. Kovaszny Baltimore 18, Maryland
1	Lehigh University Department of Physics ATTN: Professor R. J. Emrich Bethlehem, Pennsylvania
1	Pennsylvania State University Physics Department ATTN: Professor R. G. Stoner State College, Pennsylvania
1	Princeton University James Forrestal Research Center ATTN: Professor S. Bogdonoff Princeton, New Jersey
1	Princeton University Observatory ATTN: Professor Lyman Spitzer, Jr. Princeton, New Jersey
1	Stanford University Department of Mechanical Engineering ATTN: Professor D. Bershader Stanford, California
1	Syracuse University Department of Physics ATTN: Professor C. H. Bachman Syracuse, New York
1	University of California Low Pressures Research Project ATTN: Professor S. A. Schaaf Berkeley 4, California
1	University of Chicago The Enrico Fermi Institute of Nuclear Studies ATTN: Professor E. N. Parker Chicago 37, Illinois

DISTRIBUTION LIST

No. of Copies	Organization
1	University of Illinois Aeronautical Institute ATTN: Professor B. L. Hicks Urbana, Illinois
2	University of Maryland Institute for Fluid Dynamics and Applied Mathematics ATTN: Professor S. I. Pai Professor J. M. Burgers College Park, Maryland
1	University of Michigan Department of Physics ATTN: Professor Otto Laporte Ann Arbor, Michigan
1	University of Michigan Willow Run Laboratories P. O. Box 2008 Ann Arbor, Michigan
1	University of Oklahoma Department of Physics ATTN: Professor R. G. Fowler Norman, Oklahoma
1	University of Pennsylvania Moore School of Electrical Engineering ATTN: Professor S. Gorn Philadelphia, Pennsylvania
1	Dr. G. W. Anderson Sandia Corporation Sandia Base P. O. Box 5800 Albuquerque, New Mexico
1	Professor J. W. Beams University of Virginia Department of Physics McCormic Road Charlottesville, Virginia
1	Professor R. C. Binder University of Southern California Engineer Center University Park Los Angeles 7, California
1	Professor W. Bleakney Princeton University Palmer Physical Laboratory Princeton, New Jersey
1	Professor J. Lloyd Bohn Temple University Department of Physics Philadelphia, Pennsylvania
1	Professor R. G. Campbell Hartford Graduate Center R. P. I. East Windsor Hill, Connecticut
1	Mr. Paul R. Caron Research Assistant Brown University Engineering Division Providence, Rhode Island
1	Professor G. F. Carrier Division of Engineering and Applied Physics Harvard University Cambridge 38, Massachusetts
1	Dr. Eugene C. Cnare Sandia Corporation Sandia Base P. O. Box 5800 Albuquerque, New Mexico
1	Mr. Robert Dennen Armor Research Foundation Illinois Institute of Technology Center Chicago, Illinois

DISTRIBUTION LIST

No. of Copies	Organization
1	Mr. Robert W. Ellison Director, Research & Engineering National Electronics Laboratories, Inc. 1713 Kalorama Road, N. W. Washington 9, D. C.
1	Professor H. W. Emmons Harvard University Cambridge 38, Massachusetts
1	Miss Margaret W. Imbrie E. I. DuPont de Nemours and Co. Eastern Laboratory Library Drawer G. Gibbstown, New Jersey
1	Dr. G. Sargent Janes AVCO Manufacturing Corporation Advanced Development Division, Research Laboratory 2385 Revere Beach Parkway Everett 49, Massachusetts
1	Professor Jack Katzenstein The University of New Mexico Albuquerque, New Mexico
1	Dr. R. C. Maninger Librascope, Incorporated Livermore, California
1	Professor R. A. Marcus Polytechnic Institute of Brooklyn Brooklyn, New York
1	Dr. Earle B. Mayfield U. S. Naval Ordnance Test Station Michelson Laboratory China Lake, California
1	Dr. Frank W. Neilson Sandia Corporation Sandia Base P. O. Box 5800 Albuquerque, New Mexico
1	Dr. Luther E. Preuss Edsel B. Ford Institute for Medical Research Department of Physics Detroit 2, Michigan
1	Dr. A. E. Puckett Hughes Aircraft Company Culver City, California
1	Professor E. M. Pugh Carnegie Institute of Technology Department of Physics Pittsburgh, Pennsylvania
1	Dr. R. J Reithel University of California Los Alamos Scientific Laboratory Los Alamos, New Mexico
1	Mr. Zoltan Rieder Yeshiva University Graduate School of Mathematical Sciences Amsterdam Avenue & 186th Street New York 33, New York
1	Dr. Carl A. Rouse University of California Lawrence Radiation Laboratory Theoretical Division P. O. Box 808 Livermore, California
1	Dr. Daniel Schiff Raytheon Manufacturing Company Advanced Development Laboratory Government Equipment Division Waltham, Massachusetts

DISTRIBUTION LIST

No. of Copies	Organization
1	Dr. G. T. Skinner Cornell Aeronautical Laboratory, Inc. 4455 Genessee Street Buffalo 5, New York
1	Mr. W. L. Staff Lockheed Aircraft Corporation Missiles and Space Division Palo Alto, California
1	Dr. Alvin Tollestrup California Institute of Technology Pasadena, California
1	Dr. T. J. Tucker Sandia Corporation Sandia Base P. O. Box 5800 Albuquerque, New Mexico
1	Mr. E. E. Walbrecht Picatinny Arsenal Explosive Research Section Dover, New Jersey
1	Dr. Francis H. Webb California Institute of Technology Pasadena, California
1	Dr. Victor Wouk, President Electronic Energy Conversion Corporation Box 86 New York 29, New York
1	Dr. L. Zernow Aerojet-General Corporation Azusa, California

AD Accession No.
Ballistic Research Laboratories, APG
CORRELATED ELECTRICAL AND OPTICAL MEASUREMENTS OF EXPLODING WIRES
F. D. Bennett, H. S. Burden and D. D. Shear

BRL Report No. 1133 June 1961

DA Proj No. 503-03-009, OMSC No. 5210.11.140
UNCLASSIFIED Report

UNCLASSIFIED

Aerodynamics - Testing equipment
Exploding wires - Measurements

Description is given of a high-resolution streak camera and of an experimental method whereby streak camera records and electrical measurements of exploding wires may be accurately correlated in time. Composite data together with derived values of resistance, power and energy are given for 4 and 5 mil Cu wires at several voltages. These data are compared with the experimental and theoretical results of other workers. From the comparison a coherent model of the exploding wire phenomenon emerges which differs in some details, particularly those having to do with electric arc formation, from models proposed earlier. The transfer of energy from electrical to fluid mechanical form is discussed as are problems having to do with formation of the shock waves.

AD Accession No.
Ballistic Research Laboratories, APG
CORRELATED ELECTRICAL AND OPTICAL MEASUREMENTS OF EXPLODING WIRES
F. D. Bennett, H. S. Burden and D. D. Shear

BRL Report No. 1133 June 1961

DA Proj No. 503-03-009, OMSC No. 5210.11.140
UNCLASSIFIED Report

UNCLASSIFIED

Aerodynamics - Testing equipment
Exploding wires - Measurements

Description is given of a high-resolution streak camera and of an experimental method whereby streak camera records and electrical measurements of exploding wires may be accurately correlated in time. Composite data together with derived values of resistance, power and energy are given for 4 and 5 mil Cu wires at several voltages. These data are compared with the experimental and theoretical results of other workers. From the comparison a coherent model of the exploding wire phenomenon emerges which differs in some details, particularly those having to do with electric arc formation, from models proposed earlier. The transfer of energy from electrical to fluid mechanical form is discussed as are problems having to do with formation of the shock waves.

AD Accession No.
Ballistic Research Laboratories, APG
CORRELATED ELECTRICAL AND OPTICAL MEASUREMENTS OF EXPLODING WIRES
F. D. Bennett, H. S. Burden and D. D. Shear

BRL Report No. 1133 June 1961

DA Proj No. 503-03-009, OMSC No. 5210.11.140
UNCLASSIFIED Report

UNCLASSIFIED

Aerodynamics - Testing equipment
Exploding wires - Measurements

Description is given of a high-resolution streak camera and of an experimental method whereby streak camera records and electrical measurements of exploding wires may be accurately correlated in time. Composite data together with derived values of resistance, power and energy are given for 4 and 5 mil Cu wires at several voltages. These data are compared with the experimental and theoretical results of other workers. From the comparison a coherent model of the exploding wire phenomenon emerges which differs in some details, particularly those having to do with electric arc formation, from models proposed earlier. The transfer of energy from electrical to fluid mechanical form is discussed as are problems having to do with formation of the shock waves.

AD Accession No.
Ballistic Research Laboratories, APG
CORRELATED ELECTRICAL AND OPTICAL MEASUREMENTS OF EXPLODING WIRES
F. D. Bennett, H. S. Burden and D. D. Shear

BRL Report No. 1133 June 1961

DA Proj No. 503-03-009, OMSC No. 5210.11.140
UNCLASSIFIED Report

UNCLASSIFIED

Aerodynamics - Testing equipment
Exploding wires - Measurements

Description is given of a high-resolution streak camera and of an experimental method whereby streak camera records and electrical measurements of exploding wires may be accurately correlated in time. Composite data together with derived values of resistance, power and energy are given for 4 and 5 mil Cu wires at several voltages. These data are compared with the experimental and theoretical results of other workers. From the comparison a coherent model of the exploding wire phenomenon emerges which differs in some details, particularly those having to do with electric arc formation, from models proposed earlier. The transfer of energy from electrical to fluid mechanical form is discussed as are problems having to do with formation of the shock waves.